Detecting seasonal variation of antifreeze protein distribution in Rhagium mordax using immunofluorescence and high resolution microscopy

Buch, Johannes Lørup; Ramløv, Hans

Detecting seasonal variation of antifreeze protein distribution in *Rhagium mordax* using immunofluorescence and high resolution microscopy

J. L. Buch[a,*], H. Ramløv[a]

[a]*Department of Science and Environment - Roskilde University. Universitetsvej 1, 4000 Roskilde, Denmark.*

Abstract

Larvae of the blackspotted pliers support beetle, *Rhagium mordax*, were collected monthly, for the duration of 2012 and fixed. The larvae were embedded in paraffin wax and sectioned. Using fluorophore-coupled antibodies specific to the *R. mordax* antifreeze protein, RmAFP1, sections were visualised with UV reflected light microscopy. An automated software analysis method was developed in order to discard autofluorescence, and quantify fluorescence from bound antibodies. The results show that *R. mordax* cuticle and gut exhibit a higher degree of fluorophore-bound fluorescence during summer, than in the cold months. It is hypothesised that *R. mordax* stores RmAFP1 in, or near, the fat body during times when freeze avoidance is not needed. [1]

Keywords: antifreeze protein, immunofluorescence, microscopy, detection, *Rhagium mordax*, cross section, image analysis

---

*Corresponding author

Email addresses: `jloerup@gmail.com` (J. L. Buch), `hr@ruc.dk` (H. Ramløv)

[1]Abbreviations: DAPI, 4',6-diamidino-2-phenylindole (blue, 461 nm); FITC, ́Fluorescein isothiocyanate (green, 518 nm); TRITC, Rhodamine (red, 580 nm)

1. Introduction

A fundamental aspect of the temperate climate is its seasons. Terrestrial animals inhabiting this environmental zone, must therefore be able to cope with large seasonal variations in temperature, light, humidity and snow cover. During winter, the northern regions of the temperate zone may reach temperatures well below -10°C [22] [24], while summers may be above 20°C [14] [18].

Organisms vary in their response to cold and freezing conditions. Some are tolerant to freezing of their body fluids, while others must avoid such freezing. Insects may have a variety of behavioural responses, to initially avoid the cold [16] [14], but evolution has in many cases favoured the adaptation of a physiological cold response [19] [13]. In overwintering insects the external environment can produce conditions that, put the organism in danger of inoculative freezing [12]. As the environment cools, environmental ice may start to form from condensed water, and contact with such ice could be fatal for a freeze avoiding organism. Also, as insect larvae often have partly digested plant remains in their gut lumen, this internal environment may freeze, making the whole organism susceptible to inoculative freezing from the inside. As such, an emptying of the gut is often observed in larvae preparing to overwinter[18].

Freeze avoiding insects often employ a certain group of biological antifreeze agents called antifreeze proteins (AFP)[2], as well as colligative antifreeze compounds such as polyols[25], free amino acids[14] and inorganic salts [18].

When water freezes, solutes are excluded from the growing crystal, leading to a sharp concentration gradient near the crystal surface. This process is believed to be one of the main causes of tissue damage in freezing organisms [7] [1]. By inhibiting inoculation and growth of ice crystals in the body fluids, AFP's can essentially extend the period of

---

[2]As more intricate knowledge about the mechanism of these proteins have become available in recent years, they are often referred to as **I**ce **B**inding **P**roteins or **I**ce **S**tructuring **P**roteins

time before permanent damage occurs from freezing of the tissues.

A study by Olsen *et al.*, 1998, [12] showed that AFP distribution varied in tissue sections from *Dendroids canadensis* larvae as a function of season. In their immunofluorescence study [12] they observed that during winter the integument was bright from AFP-bound fluorescence, while the integument from summer larvae showed a much smaller degree of fluorescence from AFP binding. This indicated that the amount of tissue-bound AFP varies with season, and that it is strongest during winter. *R. mordax* is a freeze avoiding coleopteran, whose larvae can be found overwintering beneath the bark of rotting beech tree trunks and stumps [18]. This micro environment provides some protection from convective cooling, as well as ice crystal inoculation from surface snow or ice.

However, a previous study on the seasonal variation of AFP in *R. mordax*, by Wilkens and Ramløv [18], observed that larvae hemolymph showed thermal hysteresis activity (THA) all year, but that TH was highest during the coldest months. It was hypothesised that *R. mordax* primarily avoids freezing through AFP production, and that the synthesis of osmolytes was of secondary importance. The sister species *Rhagium inquisitor* accumulates large amounts of osmolytes, such as glycerol, during winter [23], but its distribution in general is higher north, and thus colder during winter. *R. mordax* is adapted to a warmer climate, and accumulates colligative cryoprotectants to a much smaller degree [18]. *R. mordax* can thus spend less energy on the maintenance of high hemolymph osmolality [17], and extend its growing season compared to its sister species *R. inquisitor*. A study of the thermodynamic stability of RmAFP1, the primary AFP found in *R. mordax* [5], showed that RmAFP1 has a melting point of 28.5 °C, but that it had exceptionally strong refolding capabilities. This lends credibility to the hypothesis that RmAFP1 has a long half-life in *R. mordax*, and that antifreeze activity can be

detected year round because of this.

In earlier studies it was determined that the fat bodies of larvae from *D. canadensis* [20] [3] and *Tenebrio molitor* [21] [4] were the primary production site of AFP. The fat body of *T. molitor* is filled with protein-rich granules, first observed by Easton & Horwath in 1994 [4]. These granules are immunologically active for Tm 12.86, a *T. molitor* specific AFP. In 1996, Horwath *et al.* [8], observed an accumulation of Tm 12.86 in these granules, during summer. During winter, the granules had been emptied for Tm 12.86, presumably because of release of cryoprotectants to the hemolymph. The fat body in insects is closely connected to both the integument and the gut. Due to its role in energy metabolism and AFP synthesis in *T. molitor* [21] and *D. canadensis* [20], the tissues connected to the fat body are therefore of great interest, when seeking to determine seasonal variations in AFP levels.

In two previously unpublished studies of AFP localisation in *Zoarces viviparus* [9] and *R. mordax* [10] it was confirmed that the immunofluorescence method used in this paper was functional, but needed to be expanded upon. It was further determined that, AFP distribution in the cuticle and gut epithelium of *R. mordax* did not differ significantly between winter (Figure 2a) and summer (Figure 2b) months, which is in stark contrast to the clear seasonal variation seen in 1998 by Olsen *et al.* in larvae of *D. canadensis* [12]. If anything, the amount of fluorescence during summer seemed higher than in winter in Figure 2. This discrepancy was the primary motivation, for the present study. Previous immunofluorescence micrographs of *R. mordax* larvae (Figure 2) were all non-adjacent images, taken at various points of interest. This meant that limited structural information about the cross section could be extracted. The field of view was simply too narrow. This study expands upon the technique by using several hundred micrographs, and stitching them together, forming large composites of whole larva cross sections. The goal is a greater perspective on the possible seasonal variation in tissue

4

distribution of AFP.

Based on the information presented here, the working hypothesis for this study is that, the amount of RmAFP1 associated fluorescence in *R. mordax* larvae will decrease as ambient temperature increases, as seen in *D. canadensis*. This is especially expected to be the case in the cuticle, and gut epithelium, as these two tissue types are involved in prevention of inoculative freezing.

2. Materials and methods

2.1. Capture and fixation of specimens

Larvae of *R. mordax* were collected once a month from February 2012 until January 2013 in Boserup Forest near Roskilde, Denmark. By collecting larvae for a whole year, every season is represented in the data set. A temperature logger was set up at the forest location, logging both the tree stump temperature beneath the bark and the air temperature. See Figure 1 for temperatures throughout 2012. Larvae were located by removing decomposing bark from stumps of beech trees that had been cut down a few years earlier. Larvae were transported back to the laboratory in 2 ml Eppendorf tubes covered with perforated parafilm to ensure airflow, inside an insulating styrofoam box. Larvae were placed in embedding cassettes (Klinipath 2020) for easier storage. Larvae were fixed using FineFix (HD Scientific ML 70147) and kept at 4°C until further processing. See Table 1 for an overview of the experiments.

Table 1

2.2. Tissue sectioning

The fixed larvae were cut with a scalpel to allow better fluid penetration and dehydrated in a series of increasing concentrations of ethanol and finally xylene. The dehy-

5

drated larvae were then infiltrated by molten paraffin wax (Thermo Scientific 6774006) at 60°C. Hardened blocks of paraffin wax and larvae were mounted on a Biocut 2030 microtome, and cut at 5 µm thickness. Sections were transferred to a floatation bath (Agar Scientific, L4136) filled with distilled water kept at 45-50 °C, and allowed to expand and stretch out for a few seconds before being collected onto a polysine coated glass slide (Agar Scientific L4345). Polysine slides were air dried and gently wiped around the cross sections. They were then allowed to anneal in a 40°C drying chamber for at least two hours. See Sup1 in the supplementary materials for a detailed protocol.

2.3. Tissue staining

Paraffin wax was removed by xylene submersion, and the tissue sections were rehydrated by submerging in decreasing concentrations of ethanol in water. For each batch of immunofluorescence stained tissue sections, one or two sections were also prepared for staining with hematoxylin and eosin. The main purpose of these HE stains was to help identify distinct internal anatomical structures, that may not have been visible using only UV-reflected light. Using a light polarizer, the cuticle and gut were identified in HE stains. Their unique light pattern was used as identification of tissue in the transparent immunofluorescence stains. The two staining procedures share the same 4-step protocol used for dehydration, embedding, sectioning and rehydration. See Sup2 in the supplementary materials for a detailed protocol.

2.4. Antibody production

Primary antibodies against the antifreeze proteins found in *R. mordax* were raised in rabbits against *R. mordax* AFP isoform 1 [5] and purified from serum by BioGenes GMBH. The primary antibodies were polyclonal, but this was regarded an advantage rather than an issue, due to the very subtle differences between natural AFP found in *R. mordax* and the protein produced in the laboratory, primary sequence detailed by

Friis and Kristiansen [6] [11]. Antibodies were produced in 2011 and kept at -20°C in aliquots to avoid freeze-thaw cycles. The secondary antibody used for this project was a goat-raised anti-rabbit monoclonal IgG with the Alexa Fluor 488 (Molecular Probes A-11070) tag added. To avoid excessive unspecific binding, only the pepsin-cleaved F(ab') part was used.

2.5. Data capture and -treatment

Immunofluorescence data was captured using an Axio Imager.M2m (Carl Zeiss AG, Oberkochen, Germany) setup. All of the subjects were photographed at TRITC, FITC and DAPI (red, green, blue, respectively) wavelengths, except for the larvae collected in March, June, September and October, which were only photographed in TRITC and FITC. The image-capture was performed using the same wattage on the UV lamp and with very little temporal spacing. The shutter on the lamp was closed between photographs to ensure the least amount of photobleaching of the bound fluorophores. All images were captured monochromatically, and coloured as part of the software post-processing. The final images produced in this study are all composites, stitched together from 20-50 high magnification micrographs, using the stitching functionality in the free image analysis software, FIJI [15] [3]. See Sup4 in the supplementary materials for details, as well as a graphical overview (Figure S2). Results of gut epithelium and cuticle were extracted and processed from respective parts of the whole larva cross sections.

2.6. Autofluorescence

Many biological structures have inherent and unavoidable interactions with UV-light [2]. This phenomenon is known as autofluorescence. It is crucial to take these interactions into account, as to not obtain data that are essentially only false positives. Alexa Fluor 488, the fluorophore used in this study, has an emission-maximum which resembles

---

[3]Fiji is just ImageJ http://fiji.sc/

an FITC (green) fluorophore. This means that AFP-bound fluorescence can be observed as bright green fluorescence in the micrographs. In this study, every microscopic field of view (FOV) was captured in one or two different wavelengths, in addition to FITC. These were in all cases TRITC (red) and in some cases DAPI (blue). In the image processing that yielded the final results, areas of significant red and blue autofluorescence were subtracted from the green fluorescence. This was to reduce the amount of falsely positive fluorescence in the final results. Any green fluorescence that occupies the same area as autofluorescence in the red and blue, is automatically removed. Information is lost during this process, but the remaining image only contains AFP-bound fluorescence. For images not containing DAPI-data, the image processing macro automatically detects this, and removes autofluorescence using TRITC only. One of the final quantifiable results is the percentage of positive fluorescence compared to the total amount of green fluorescence, which is called *area*. At *area* = 0, all the green fluorescence in the cross section is autofluorescence. At *area* = 100, none of the green fluorescence is autofluorescence. The other result parameter is *intensity*, which is average fluorescent intensity of the positive, green fluorescence. The two parameters, *area* and *intensity*, may vary independently of one another. An increase in *area* indicates a more general trend than an increase in *intensity*, which may indicate a higher concentration of AFP in a certain spot. The full analysis script is available at https://github.com/pechano/immuno and in Sup5 in the supplementary materials, where a graphical overview can also be found (Figure S3).

3. Results

The temperature data from Boserup forest, 2012, are shown in Figure 1. Four probes were installed at the forest location, but only three survived for the duration of the study. First and last cold- (<4 °C) and freezing events (<0 °C) are marked on Figure 1. There are approximately six months between freezing events at the forest location (April 8. -

October 28.), and about five months between cold events (May 7. - October 26.), where the temperature stays above 4 °C. On October 20, the temperature is 16 °C, only eight days before the first freezing event of 2012. The red line in Figure 1 is THA of *R. mordax* hemolymph, measured by Wilkens and Ramløv in 2003 [18]. An inverse relationship between temperature and hemolymph THA can be seen in Figure 1.

FIGURE1

The first immunofluorescence result presented here, is from a previously unpublished study [10], which was the inspiration for the present study. In Figure 2 two micrographs showing summer (2b) and winter (2a) can be seen. They are stained with the same fluorophore used in the present study, Alexa Fluor 488, which is green. The single arrows point to the epicuticle, and the double arrows point to the epidermis, underneath the cuticle. On the summer micrograph, the fat body tissue attached to the cuticle is bright with fluorescence. This was the first indication that AFP concentration in the tissue is higher during summer, than during winter.

FIGURE2

Before quantification of immunofluorescence was performed, the micrographs from each individual larval cross section were stitched together. Figure 3 shows a stitched larval cross section from December 2012. The cross section is stained with Alexa Fluor 488 (FITC, green). The star marks the gut lumen, where not much is seen, as the larvae empty it during winter. The spongy tissue which the double arrows sit on top of, is part of the fat body. The quantification of fluorescence was performed on cross sections such as the one seen in Figure 3, and data from specific tissues were extracted from this type of image.

FIGURE3

Figure 4 shows four sample images produced by the software analysis method. The cross sections were stitched together from approximately 80 smaller images. Each image is therefore approximately 30-40 megapixels in size. The top panel contains a sample from an immunostained cross section, before and after image processing. After processing (4b), the green outline represents AFP-bound fluorescence that cannot be disqualified due to autofluorescence. The bottom panel shows a control experiment, also before and after processing. In the control cross section with no Alexa Fluor 488, the entire image is removed due to autofluorescence. The processing method used here, is able to separate immunostained cross sections from control cross section with no fluorophore. The visual difference is striking, but also quantifiable. In this case, 69% of the green fluorescence in fig. 4a remains after processing (fig. 4b). The *area* result parameter for this particular cross section is therefore 69. For comparison, the *area* of the control cross section (fig. 4c+4d) is 2%. The type of quantification shown in Figure 4 was performed on all larval cross sections and the results can be seen in Figure 6. For the full high-resolution image gallery of control and non-control experiments, see https://imgur.com/a/9bmuN and https://imgur.com/a/EHSc3, respectively.

FIGURE4

Figure 5 shows the quantified positive *area* and *intensity* in several control cross sections, compared to an immunostained cross section from May. The control experiments were a collection of cross sections from January and August, containing either no primary or no secondary antibodies, resembling the cross section seen in fig. 4c. The background *intensity* for the entire dataset is therefore 57 ± 1.02, and the baseline for *area* is almost zero. By using the *area* and *intensity* result parameters, control- and immunostained cross sections are shown to be significantly different ($p<0.05$). The visual

inspection in Figure 4 and the statistical test in Figure 5 show that the image processing method developed for this study, works as intended.

FIGURE5

Whole cross sections from each month were subject to the analysis seen in Figure 4, and the results are plotted in Figure 6. The blue dots are the *area* parameter and the orange dots are *intensity*. The immunofluorescence results are plotted on the left y-axis. The month mean temperature is plotted as a red line in Figure 6, but on the right y-axis. No significant correlations could be observed. This was unexpected, as previous studies have shown seasonal variation of AFP in both *D. canadensis* [12], *T. molitor* [8] and *R.mordax* [18]. It was determined that whole larval cross sections were not a good target for analysis, as subtle differences are drowned out by the inherent variations in the larvae. A more focused approach, using the analysis method on images of gut epithelium and cuticle only, was initiated.

FIGURE6

Smaller images containing gut epithelium and cuticle were extracted from the large composite images, and run through the same analysis method. Examples of the extracted images can be seen in Figure 7, which shows cuticle from a December larva (fig. 7a) and gut epithelium from a February larva (fig. 7b). As the gut is always found near the middle of the cross section, it is easy to extract from larger images and include in the image analysis. The cuticle, however, spans the entire outer boundary of the cross section, so smaller sections of it had to be extracted.

FIGURE7

All results from cross sections and extracted images, were compared to mean tem-

perature and the correlation matrix is visualised in Figure 8. In Figure 8 "Cross.area" and "Cross.intensity" refer to *area* and *intensity* of the whole cross section, respectively. Significant correlations ($p < 0.05$) are marked by ellipsoids containing no numbers. The numbers in the remaining ellipsoids represent non-significant p-values from the correlation analysis. The colour indicates correlation value, from 1 (blue) to -1 (red). The narrower the ellipsoid, the stronger the correlation. All significant correlations are positive (blue), meaning that fluorescence parameters increase with temperature.

In the correlation plot seen in Figure 8, it is clear that cuticle *area* and gut *intensity* are both positively correlated with ambient temperature (top lane). This was tested with a regression analysis, and both correlations are significant, with $p < 0.05$. The small green box draws attention to a significant correlation between cuticle- and gut *area*, which indicates connection with temperature, which could not be seen in the top lane. The large green rectangle in Figure 8 draws attention to four correlations between *area* and *intensity* of cuticle and gut, to the respective counterparts in the whole cross sections. This is to be expected, since they share the same origin. It is still relevant to observe, as it validates part of the data processing method. Since the extracted images are well correlated to the cross section they came from, it indicates that the extraction method produces good representations of the whole. The cross section *area* is nearly significantly correlated to temperature, with $p = 0.057$, but will be treated instead as a statistical tendency (top lane). To summarise: Fluorescence of whole immunostained cross sections, does not vary in a temperature dependent fashion. However, it is clear that fluorescence in both gut and cuticle increases with ambient temperature. When the forest temperature increases, RmAFP1 in the cuticle distributes into a larger area, and RmAFP1 near the gut concentrates in dense areas.

FIGURE8

12

4. Discussion

To elucidate on previously unpublished findings in *R. mordax*, a new, automated data-processing approach was developed. The processing method allows for quantification of qualitative comparisons, like the one shown in Figure 2. For micrographs captured under the same conditions, it is possible to objectively compare them using the method presented in this work.

The correlations shown in Figure 8 are all positive, which means that AFP-bound fluorescence increases with temperature. This is opposite of what can be observed in cross sections of *D. canadensis* [12] and hemolymph AFP in *R. mordax* [18].

While no significant correlation can be established between temperature and either fluorescence intensity or area in whole larval cross sections, it is perhaps more surprising to see that there is no correlation between the two fluorescence parameters, *area* and *intensity* (0.41, bottom square in Figure 8). A larger relative area of positive fluorescence, does not equal high fluorescence intensity. At least not directly. This opens the possibility of fluorescence patterns, which are difficult to detect and identify. If most of the AFP-bound fluorescence is concentrated in a small area, the *intensity* will increase, but area doesn't necessarily follow. However, from Figure 8 we can see that intensity and area, of both gut and cuticle, are correlated to their respective parent parameters (*area* and *intensity*), in the whole larva cross sections. So while changes in fluorescence levels, of the larval cross sections can not be adequately explained by changes in temperature, changes in the correlated specific tissues can be explained by variations in temperature. These results indicate a storage mechanism for RmAFP1 in the tissues surrounding the cuticle and gut epithelium, much like in *T. molitor* [8].

Accurate thickness measurements of the gut epithelium and cuticle would be desirable to have in the correlation matrix, but it was not possible to obtain reliable, objective results, for the entire set. A further development of the automated analysis macro is

needed to accomplish this.

The study by Wilkens and Ramløv [18] measured TH activity in the hemolymph, while the present study specifically concerns tissue cross sections. In both cases, RmAFP1 can be observed at all time points, but the relationship between hemolymph TH and temperature, seen by Wilkens and Ramløv [18], seems to be the opposite of the results obtained in this study. Figure 1 shows the THA measured by Wilkens and Ramløv [18] and it is clear that the hemolymph concentration of AFP is negatively correlated with temperature. However, tissue abundance of AFP, may not be the same as hemolymph activity. The fluorescence pattern of tissue AFP observed in *D. canadensis* by Olsen *et al.* in 1998 [12], is also the opposite of the results presented here. The fat body connects to both the cuticle and gut, and assuming the stored proteins are immunologically active, as can be observed in *T. molitor* [8], they would result in increased IgG binding in these two tissues. This would generate the fluorescence pattern observed in the results. In *T. molitor*, an increase in AFP abundance has been observed in protein rich granules in the fat body [8], during summer. RmAFP1-rich granules were not directly observed during the present study, but the previously unpublished micrographs shown in Figure 2 indicates the presence of a similar mechanism in *R. mordax*.

It therefore seems more likely that *R. mordax* resembles *T. molitor* [8] [4], as AFP bound fluorescence increases during summer. This is only a tendency for whole larva cross sections, but a significant relationship for tissues near gut and cuticle. These relationships can be seen as significant correlations in the top panel of Figure 8.

The temperature profile of the forest location in 2012, seen in Figure 1, shows that the first freezing event of the year, happens very quickly. The temperature drops from 15°C to freezing temperatures in less than 14 days. In *D. canadensis* the response time of detectable hemolymph TH activity is 2-3 weeks [20]. The climate is known to produce sudden cold spells, even during the warmer months of the year. A clear night during

14

late summer, may produce sub-zero temperatures, even if it is just for a few hours. *R. mordax* is a freeze avoiding insect, living in the temperate forests. Being able to prepare for sudden cold spells, by effectively storing AFP near the gut and cuticle may have been strongly favoured by evolution, even if this mechanism hasn't been observed frequently. The temperature at the forest location, where larvae used in this study were collected, changed from +15 °C to freezing temperatures in a week. For unprepared ectothermic organisms, this sudden change could be dangerous. The release of stored AFP is surely faster than *de novo* synthesis. A study of the thermodynamic stability of RmAFP1, showed that the protein has a melting point of 28.5°C, but that the refolding capability was extremely high [6]. RmAFP1 is therefore partially unfolded during most of the summer. For this reason, it would seem favourable to store RmAFP1 in granules, where the unfolded fraction is not able to react idiosyncratically with hemolymph constituents. The protein rich granules reported in *T. molitor* are not directly observed in *R. mordax*, but a similar storage mechanism seems to be the case.

5. Conclusion

Through extensive image analysis of cross sections from *R. mordax* larvae, it can be concluded that there is a significant correlation between RmAFP1 and environmental temperature in, and around, gut epithelium and cuticle. This leads to the hypothesis that, *R. mordax* stores RmAFP1 in the fat body during summer, when it is not needed as a cryoprotectant.

6. Acknowledgements

7. Conflict of interest

Conflicts of interest: none

[1] Carpenter, J. F., Hansen, T. N., Jan. 1992. Antifreeze protein modulates cell survival during cryopreservation: mediation through influence on ice crystal growth. Proceedings of the National Academy of Sciences 89 (19), 8953–8957.
URL http://www.pnas.org/content/89/19/8953

[2] Chang, N., Mao, J., Lu, Y., Yang, J., Pu, Y., Zhang, S., Liu, Y., Oct. 2016. Time-resolved phosphorescent sensor array based on quantum dots for recognition of proteins. Sensors and Actuators B: Chemical 233, 17–24.
URL http://www.sciencedirect.com/science/article/pii/S0925400516305275

[3] Duman, J., Verleye, D., Li, N., Aug. 2002. Site-specific forms of antifreeze protein in the beetle *Dendroides canadensis*. Journal of Comparative Physiology B 172 (6), 547–552.
URL http://link.springer.com.molly.ruc.dk/article/10.1007/s00360-002-0284-x

[4] Easton, C. M., Horwath, K. L., Jun. 1994. Characterization of primary cell cultures derived from fat body of the beetle, *Tenebrio molitor*, and the immunolocalization of a thermal hysteresis protein in vitro. Journal of Insect Physiology 40 (6), 537–547.
URL http://www.sciencedirect.com/science/article/pii/0022191094901279

[5] Friis, D. S., Johnsen, J. L., Kristiansen, E., Westh, P., Ramløv, H., Jun. 2014. Low thermodynamic but high kinetic stability of an antifreeze protein from *Rhagium mordax*. Protein Science : A Publication of the Protein Society 23 (6), 760–768.
URL http://www.ncbi.nlm.nih.gov/pmc/articles/PMC4093952/

[6] Friis, D. S., Kristiansen, E., von Solms, N., Ramløv, H., May 2014. Antifreeze activity enhancement by site directed mutagenesis on an antifreeze protein from the beetle *Rhagium mordax*. FEBS Letters 588 (9), 1767–1772.
URL http://www.sciencedirect.com/science/article/pii/S0014579314002518

[7] Halwani, D. O., Brockbank, K. G. M., Duman, J. G., Campbell, L. H., Jun. 2014. Recombinant *Dendroides canadensis* antifreeze proteins as potential ingredients in cryopreservation solutions. Cryobiology 68 (3), 411–418.
URL http://www.sciencedirect.com/science/article/pii/S0011224014000686

[8] Horwath, K. L., Easton, C. M., Poggioli, G. J., Myers, K., Schnorr, I. L., 1996. Tracking the profile of a specific antifreeze protein and its contribution to the thermal hysteresis activity in cold hardy insects. European Journal of Entomology 93 (3), 419–433, wOS:A1996VN62700013.

17

[9] Johnsen, J. L., Mar. 2011. Localization of antifreeze proteins in the European eelpout, Zoarces viviparus, by fluorescence microscopy. Thesis, http://rudar.ruc.dk/handle/1800/6312.
URL http://rudar.ruc.dk/handle/1800/6312

[10] Johnsen, J. L., Jan. 2012. Localisation of antifreeze proteins in Rhagium mordax using immunfluorescence. Thesis, http://rudar.ruc.dk/handle/1800/7275.
URL http://rudar.ruc.dk/handle/1800/7275

[11] Kristiansen, E., Wilkens, C., Vincents, B., Friis, D., Lorentzen, A. B., Jenssen, H., Løbner-Olesen, A., Ramløv, H., Sep. 2012. Hyperactive antifreeze proteins from longhorn beetles: Some structural insights. Journal of Insect Physiology.
URL http://linkinghub.elsevier.com/retrieve/pii/S0022191012002314

[12] Olsen, T. M., Sass, S. J., Li, N., Duman, J. G., May 1998. Factors contributing to seasonal increases in inoculative freezing resistance in overwintering fire-colored beetle larvae *Dendroides canadensis* (Pyrochroidae). Journal of Experimental Biology 201 (10), 1585–1594, wOS:000074211300007.

[13] Pertaya, N., Marshall, C. B., Celik, Y., Davies, P. L., Braslavsky, I., Jul. 2008. Direct visualization of spruce budworm antifreeze protein interacting with ice crystals: Basal plane affinity confers hyperactivity. Biophysical Journal 95 (1), 333–341, wOS:000256668200033.

[14] Ramlov, H., Apr. 1999. Microclimate and variations in haemolymph composition in the freezing-tolerant New Zealand alpine weta *Hemideina maori* Hutton (Orthoptera : Stenopelmatidae). Journal of Comparative Physiology B-Biochemical Systemic and Environmental Physiology 169 (3), 224–235, wOS:000080092400010.

[15] Schindelin, J., Arganda-Carreras, I., Frise, E., Kaynig, V., Longair, M., Pietzsch, T., Preibisch, S., Rueden, C., Saalfeld, S., Schmid, B., Tinevez, J.-Y., White, D. J., Hartenstein, V., Eliceiri, K., Tomancak, P., Cardona, A., Jul. 2012. Fiji: an open-source platform for biological-image analysis. Nature Methods 9 (7), 676–682.
URL http://www.nature.com/nmeth/journal/v9/n7/full/nmeth.2019.html

[16] Schoville, S. D., Slatyer, R. A., Bergdahl, J. C., Valdez, G. A., Jul. 2015. Conserved and narrow temperature limits in alpine insects: Thermal tolerance and supercooling points of the ice-crawlers, Grylloblatta (Insecta: Grylloblattodea: Grylloblattidae). Journal of Insect Physiology 78, 55–61.
URL http://www.sciencedirect.com/science/article/pii/S0022191015000980

[17] Teets, N. M., Kawarasaki, Y., Lee Jr., R. E., Denlinger, D. L., Apr. 2012. Energetic consequences of repeated and prolonged dehydration in the Antarctic midge, *Belgica antarctica*. Journal of Insect Physiology 58 (4), 498–505.
URL http://www.sciencedirect.com/science/article/pii/S0022191011003271

[18] Wilkens, C., Ramløv, H., 2008 Jul-Aug. Seasonal variations in antifreeze protein activity and haemolymph osmolality in larvae of the beetle *Ragium mordax* (Coleoptera: Cerambycidae). Cryo letters 29 (4), 293–300.

[19] Wu, D. W., Duman, J. G., Jul. 1991. Activation of antifreeze proteins from larvae of the beetle *Dendroides canadensis*. Journal of Comparative Physiology B 161 (3), 279–283.
URL http://link.springer.com.molly.ruc.dk/article/10.1007/BF00262309

[20] Xu, L., Duman, J., Jun. 1991. Involvement of Juvenile-Hormone in the Induction of Antifreeze Protein-Production by the Fat-Body of Larvae of the Beetle *Dendroides canadensis*. Journal of Experimental Zoology 258 (3), 288–293, wOS:A1991FT00200002.

[21] Xu, L., Duman, J., Wu, D., Goodman, W., JAN-FEB 1992. A Role for Juvenile-Hormone in the Induction of Antifreeze Protein-Production by the Fat-Body in the Beetle *Tenebrio molitor*. Comparative Biochemistry and Physiology B-Biochemistry & Molecular Biology 101 (1-2), 105–109, wOS:A1992HG01900017.

[22] Zachariassen, K. E., Baust, J. G., Lee Jr., R. E., Apr. 1982. A method for quantitative determination of ice nucleating agents in insect hemolymph. Cryobiology 19 (2), 180–184.
URL http://www.sciencedirect.com/science/article/pii/0011224082901390

[23] Zachariassen, K. E., DeVries, A. L., Hunt, B., Kristiansen, E., Apr. 2002. Effect of ice fraction and dilution factor on the antifreeze activity in the hemolymph of the cerambycid beetle *Rhagium inquisitor*. Cryobiology 44 (2), 132–141.
URL http://www.sciencedirect.com/science/article/pii/S0011224002000147

[24] Zachariassen, K. E., Li, N. G., Laugsand, A. E., Kristiansen, E., Pedersen, S. A., Jun. 2008. Is the strategy for cold hardiness in insects determined by their water balance? A study on two closely related families of beetles: Cerambycidae and Chrysomelidae. Journal of Comparative Physiology B 178 (8), 977–984.
URL http://link.springer.com.molly.ruc.dk/article/10.1007/s00360-008-0284-6

[25] Zheng, X.-L., Zhou, L.-J., Lu, W., Xian, Z.-H., Yang, Z.-D., Lei, C.-L., Wang, X.-P., Dec. 2014. Cold-Hardiness Mechanisms in Third Instar Larvae of *Spodoptera exigua* Hübner (Lepidoptera: Noctuidae). African Entomology 22 (4), 863–871.
URL http://www.bioone.org.molly.ruc.dk/doi/abs/10.4001/003.022.0401

8. Figures

19

Table 1: An overview of the experiments contained in the data set. RGB means an image with all three wavelengths, while "No DAPI" lacks the blue. The control experiments were done either without primary (anti-AFP) or secondary (anti-rabbit) antibodies. The exclusion of either antibody resulted in the same autofluorescence pattern. The group of controls made with ZvAFP were shown to be strongly cross-reacting.

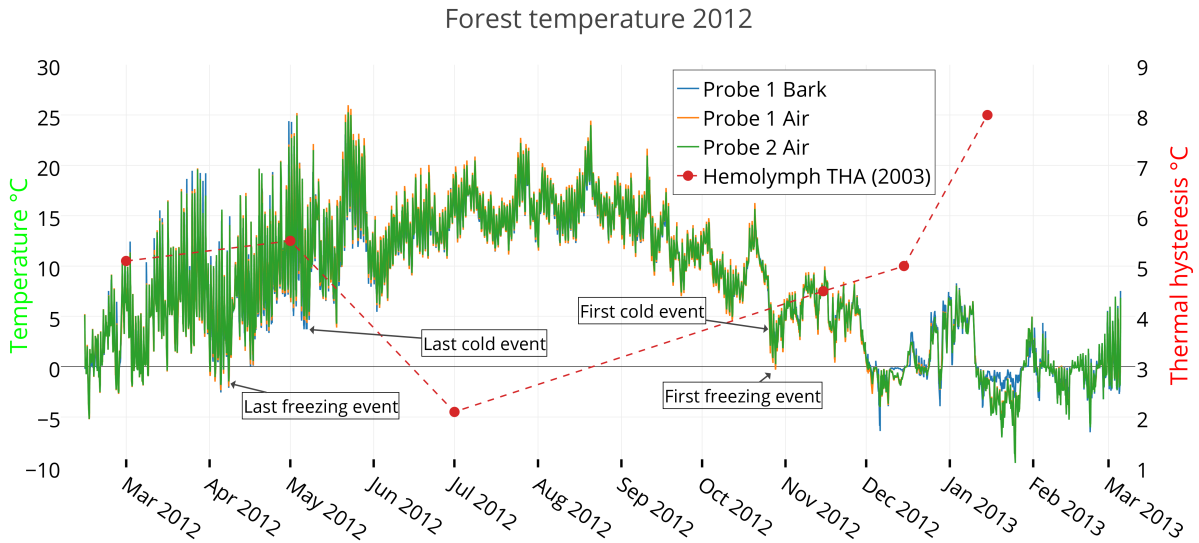| Month	RGB	No DAPI	No AFP-IgG	No rabbit-IgG	ZvAFP IgG
Feb12	x	x			
Mar12		x			
Apr12	x				
May12	x				
Jun12		x			
Jul12	x				x
Aug12	x		x	x	x
Sep12		x			
Oct12		x			
Nov12	x	x			x
Dec12	x				x
Jan13	x		x	x	x

Figure 1: Temperature in Boserup forest, when the larvae were collected. Temperatures were measured with three probes. The bark temperature was measured by sliding the thermistor in to the space between the decomposing bark and the tree stump, the same microhabitat that the larvae were collected in. Air temperatures were measured by chips in the thermologgers themselves, and therefore represent the metal housing on top of the tree stump. Freezing temperatures (<0 °C) and cold temperatures (<4 °C) are marked. The red dots represent hemolymph thermal hysteresis of *R. mordax* larvae collected in 2003 [18]. The dashed red line does not represent actual data points. An inverse relationship can be seen between hemolymph THA and temperature.

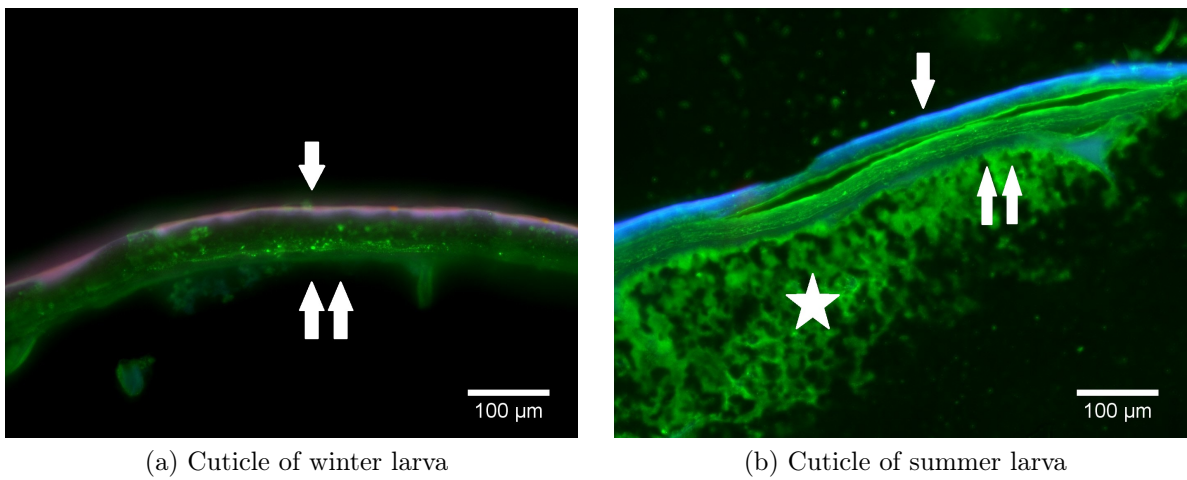(a) Cuticle of winter larva   (b) Cuticle of summer larva

Figure 2: Selected results from a previously unpublished study [10] of RmAFP1 distribution in *R. mordax*. Micrographs of *R. mordax* cuticle on larvae collected during winter 2a and summer 2b. Larvae were stained with a green antibody, specific to the most abundant *R. mordax* AFP isomer, RmAFP1. The single arrow points at the epicuticle, the double arrows point to the epidermis. In the summer larva (2b) the star marks the fat body near the epidermis. A bright green AFP-bound fluorescence can be seen in both micrographs, but the fluorescence below the cuticle seems stronger during summer. Scale bars are 100 µm.
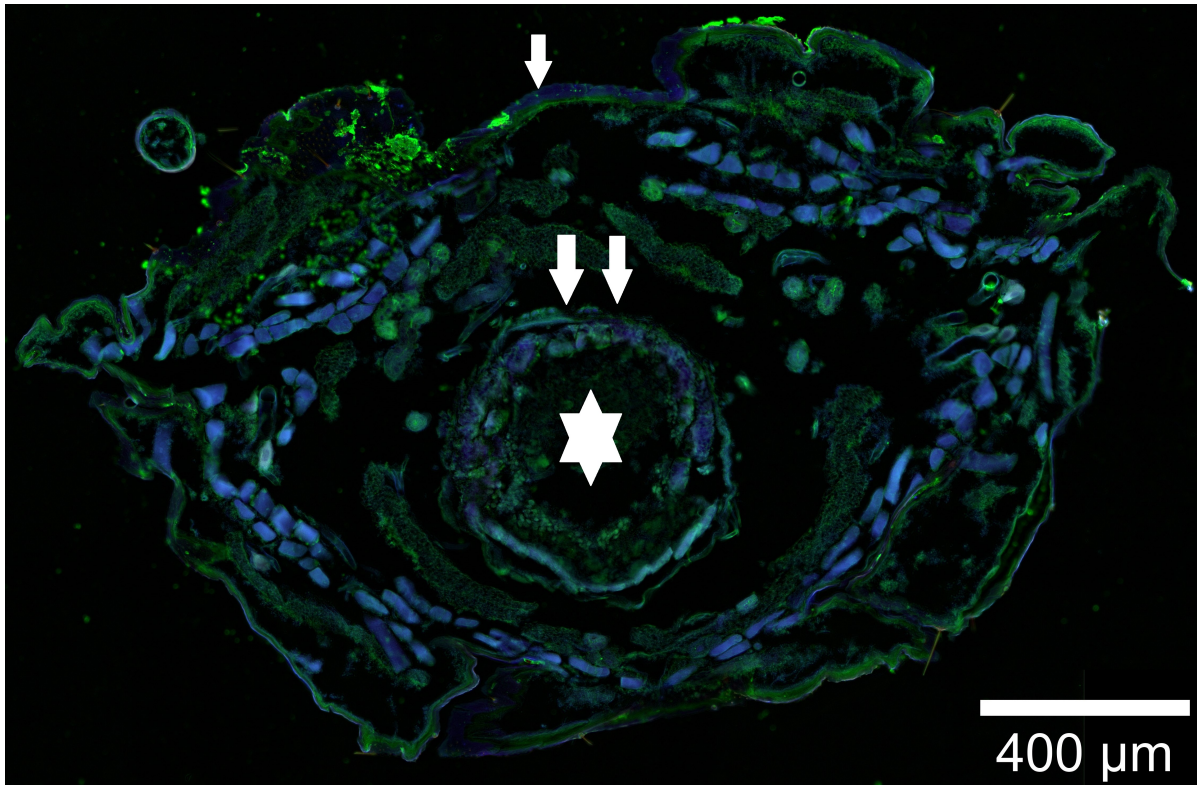
Figure 3: Stitched image of a larval cross section from December 2012. This composite image was made from 22 micrographs. The final resolution is 13.5 megapixels. The cross section was stained with Alexa Fluor 488, and AFP-bound fluorescence is therefore green. The single arrow points to the cuticle, which is often seen with a bright autofluorescent outline. The double arrows point to the gut epithelium, and the star marks the gut lumen. The data on cuticle and gut fluorescence seen later in this study, were extracted from images such as this.
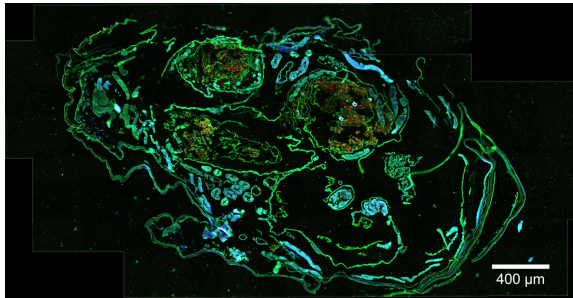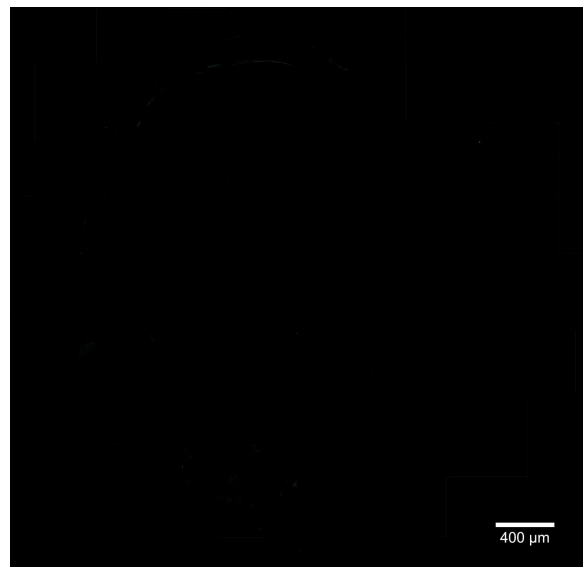
(a) August cross section
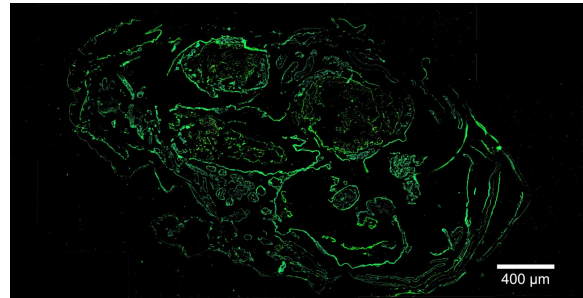
(b) August positive fluorescence
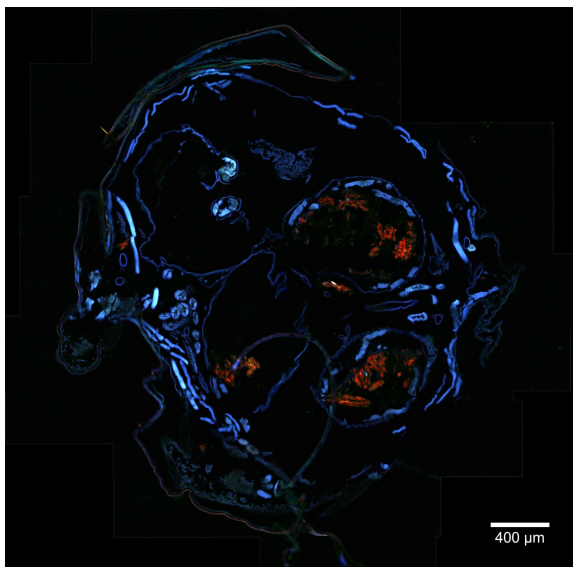
(c) August control cross section (No secondary IgG)

(d) August control positive fluorescence (No secondary IgG)

Figure 4: Immunostained cross section analysis (a+b) vs. control with no secondary IgG (c+d). Initial images (a+c) have been processed using the automated method which removes autofluorescence, and the processing results are seen in the right column (b+d, respectively). In areas where red and/or blue fluorescence is significant, the green fluorescence is removed to reduce the risk of false positives. The initial image of the immunostained cross section (a) shows bright green fluorescence throughout. The red areas with strong red fluorescence are contents of the gut. Areas showing blue fluorescence are often muscle fibers. The green area in (b) is only positive fluorescence. The green outline in (b) indicates that the antibodies are bound in the epithelium. The lack of green fluorescence in (c+d) indicates that the control experiment works as intended. With no fluorescent probes present, the initial image (c) only consists only of autofluorescence. In the processed control (d), there is no positive fluorescence visible, which confirms that no un-specific binding has taken place. Colour levels have been increased threefold for publication. Scale bars are 400 µm.
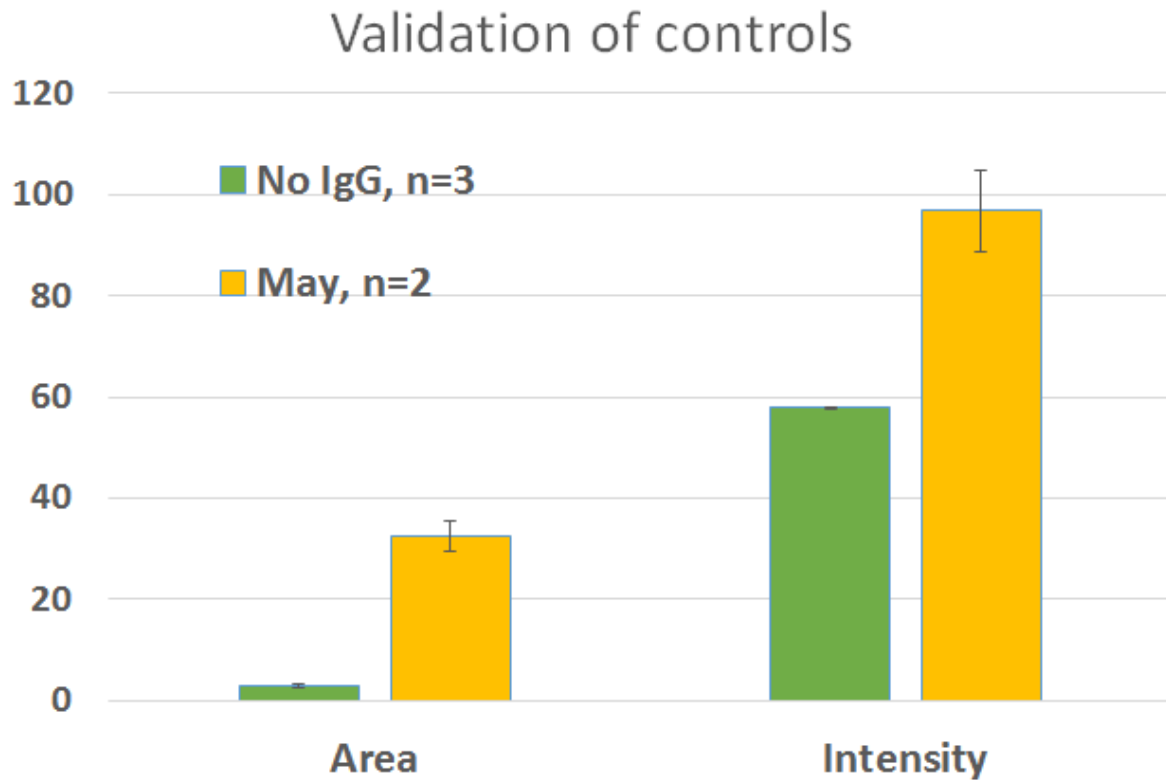
Figure 5: Quantified positive *area* and *intensity* of immunostained- and control cross sections. Data was produced using the same image processing macro, meaning autofluorescence has been removed. Green bars are controls without IgG and the yellow bars are immunostains from May, for the sake of comparison. The n denotes number of replicates. Bars are shown $\pm$ SD. The y-axis is both percentage and intensity. The control *area* and *intensity* parameters (green) are significantly different from immunostained cross sections from May (yellow) ($p < 0.05$.)

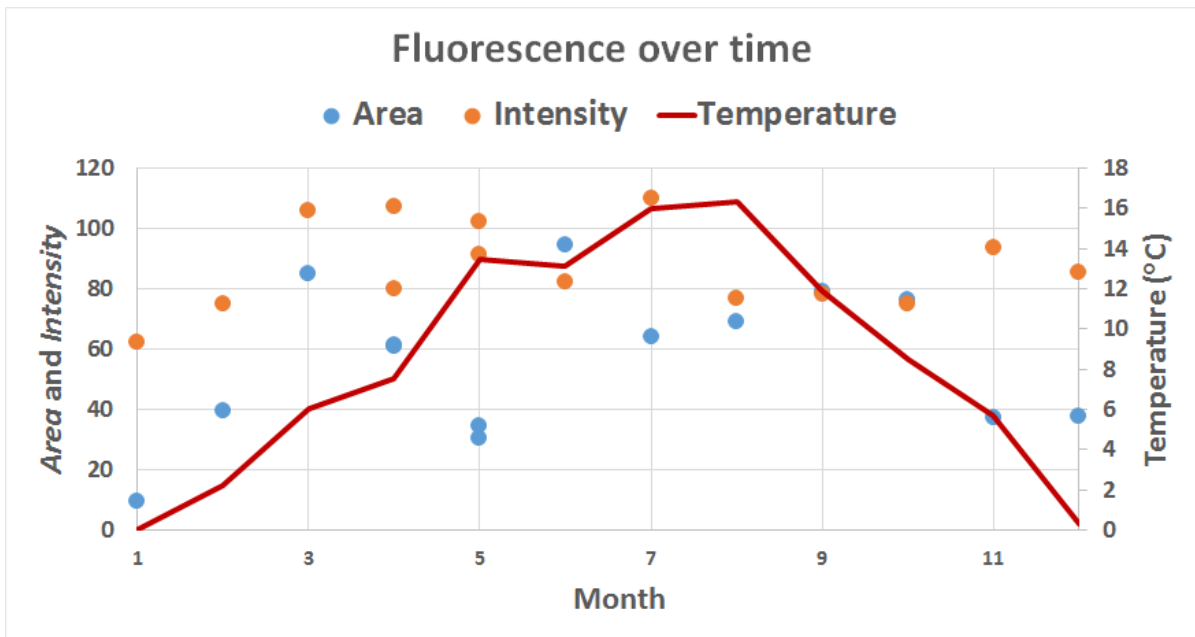Figure 6: Plot of temperature (red line), cross section fluorescence *intensity* (orange dots) and cross section fluorescence *area* (blue dots), throughout 2012. The x-axis is month of the year, left y-axis is *area* percentage and *intensity* values. The right y-axis is temperature. The variation is too great, and no correlation can be observed between any of the parameters.

(a) Cuticle from December larva
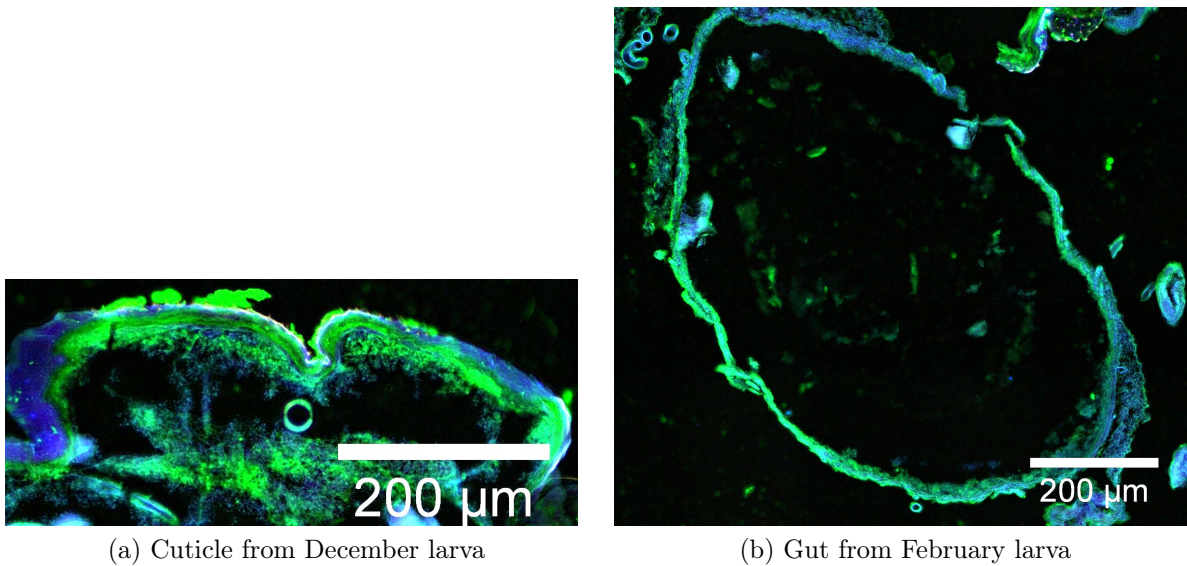

(b) Gut from February larva

Figure 7: Examples of images extracted from whole immunostained cross sections. The left image shows larval cuticle, digitally extracted from a cross section of a larva collected in December. The right image shows the gut lining and lumen, from a larva collected in February. Both images are prior to processing, so no autofluorescence has been removed.
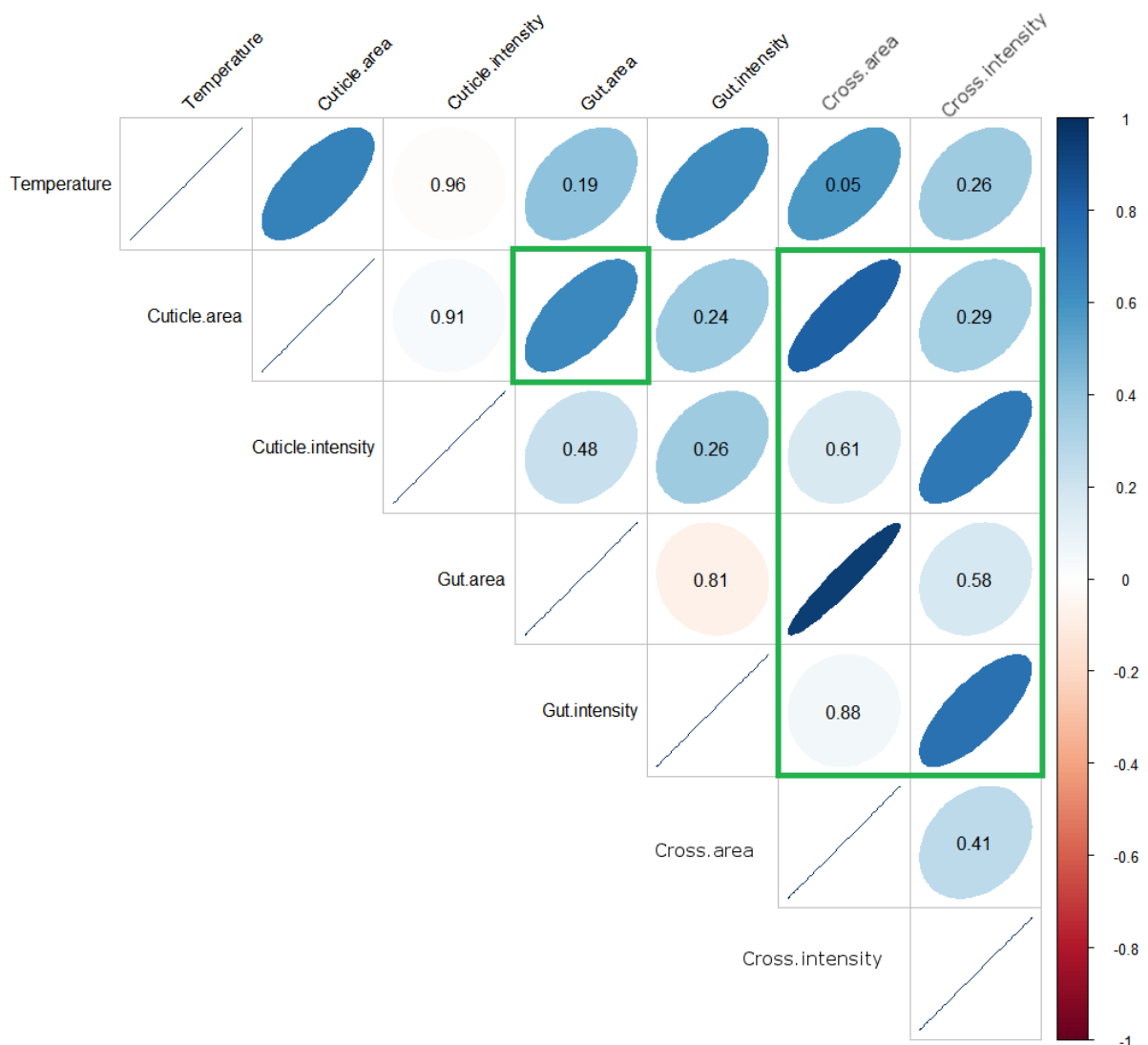
Figure 8: Correlation matrix of all cross sections (Cross.area, Cross.intensity), gut- + cuticle images and temperature. The colour scale indicates the correlation factor, r (blue = 1, positive correlation; red = -1, negative correlation). The numbers inside the squares are p-values of insignificant correlations. Significant correlations are: p<0.05. The narrow ellipsoids with no numbers indicate significant correlations, so the thinner the ellipsoid, the stronger the correlation. Noteworthy correlations are emphasised with green rectangles: The small green box notes a correlation between cuticle- and gut *area*, which indicates that these two types of tissue share some functionality. The large green rectangle shows significant correlations between gut- and cuticle fluorescence and fluorescence in the whole cross section. This was expected, as it validates the image extraction procedure.

1 **Supplementary Materials: Detecting seasonal variation of**
2 **antifreeze protein distribution in *Rhagium mordax* using**
3 **immunofluorescence and high resolution microscopy**

Sup1. Tissue sectioning

5 A short graphical overview of the cross section preparation method can be seen in
6 Figure S1, and a full protocl can be found below.
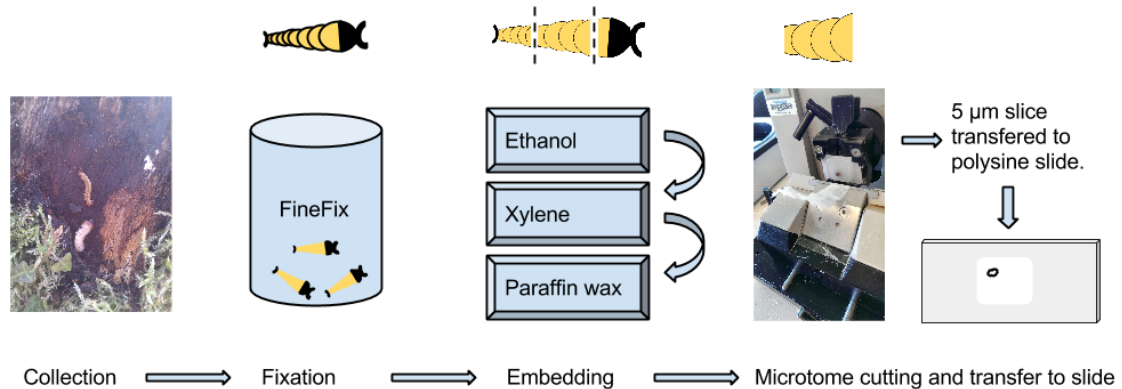
Figure S1: Overview of the slide preparation method. Larvae were captured, fixed, dehydrated, embedded in parrafin wax and sectioned on a microtome in 5 µm slices. Sections were transferred to polysine slides using a floatation bath. The glass slides containing the cross sections were allowed to anneal and dry for two hours before moving on.

```
1: Dehydration of fixed tissue

Larva is removed from FineFix and cut twice perpendicular to the
↪   bilateral axis using a scalpel. As the fixed larvae can be very
↪   soft, it is important to slice and not push the scalpel through.

The three pieces of larva are transferred to increasingly concentrated
↪   solutions of ethanol while being gently shaken (IKA Labortechnik KS
↪   125 B S1 Orbital Shaker).

- 80\% ethanol, one hour
- 95\% ethanol, two times, one hour each
- 100\% ethanol, three times, one hour each

Exces ethanol is removed with xylene:
```

Xylene is toxic and should be handled under fume hood.

- Pure xylene, three times, one hour each

2: Embedding in paraffin wax

Tissue is infiltrated by molten paraffin wax at ~60°C. This can be done
↪ in an embedding cassette while placed in the embedding mold (Thermo
↪ Scientific 6401016), but the cassette must be removed before the
↪ last infiltration as this is the paraffin that is allowed to harden.
↪ The paraffin wax is kept warm at the bottom of a Thermolyne Type
↪ 16500 Dri-Bath covered with aluminium foil and styrofoam.

- Molten paraffin wax, 90 minutes

Tissue sample is moved to a new mold with molten wax and left on the
↪ heater over night to ensure 100\% infiltration.

- Molten paraffin wax, over night (>12 hours)

The mold is filled with clean paraffin wax one last time, and allowed to
↪ solidify. The block of paraffin and tissue is then ready for
↪ sectioning on the microtome. Note that the paraffin wax should not
↪ be allowed to harden slowly, as crystals may form. Room temperature
↪ around 20°C should be sufficiently cool.

- Remove tissue from cassette and place in base mold filled with molten
↪ paraffin.

Wait for the tissue to settle and the paraffin wax to become completely
↪ fluid again. The best way to position the larval tissue is by having
↪ the bilateral axis perpendicular to the bottom of the mold. This
↪ way, every section will contain more or less the same tissue and be
↪ easier to compare.

- Remove mold from heater and allow the wax to harden.

3: Cutting and mounting

Mount paraffin block in Biocut 2030 microtome and cut sections of 5 μm
↪ at a 5° angle.

```
Sections are transferred to a flotation bath (Agar Scientific, L4136)
↪    filled with deionized water at 45-50 °C using metal instruments
↪    coated with paraffin.

Expanded sections are quickly and carefully collected directly onto
↪    polysine slides (Agar Scientific L4345) from the flotation bath.

Slides are dried in an oven set to 40°C for at least two hours.

4: Removal of paraffin and rehydration

Slides are placed in a slide staining holder (Bio Optica, 10-42) for
↪    faster processing. Each step is carried out in a separate slide
↪    staining dish (Bio Optica, 10-30).

- Slides are incubated in xylene for 10 minutes to remove paraffin wax.

Rehydration of tissue is done using decreasing concentrations of
↪    ethanol:

- 100\% ethanol, two minutes
- 95\% ethanol, one minute

Slides are rehydrated with distilled water

 - Distilled water, one minute.

From now on, the slides should not be allowed to dehydrate, as it can
↪    obscure antigens.

The tissue sections are now ready for immunostaining or HE staining.
```

1 Sup2. Immuno staining

2   Following below, are the step-by-step staining protocols used in this study.

```
1: Blocking and staining

- Mark area around section with PAP pen (Agar Scientific, L4197S) to
↪    avoid runoff of antibodies or blocking solution.

- Place slides in steel incubator (Agar Scientific, L4474).
```

- Add 100 µl of blocking solution per slide and incubate at room
  ↪ temperature for 30 minutes with the lid closed.

Drain blocking solution from slides by tilting and gently touching the
  ↪ surface of the water with lens paper.

- Add 100 µl of primary antibody per slide. Incubate at 4°C overnight.

- Wash slides in 1x TBS 4 times, 5 minutes each.

- Rinse once with 5\% BSA in TBS, 5 minutes.

Secondary antibody contains a photosensitive region, so do the following
  ↪ steps should be performed in the dark, if possible.

- Add 100 µl secondary antibody and incubate at room temperature for 30
  ↪ minutes.

- Wash with 1x TBS 4 times, 5 minutes each.

2: Mounting and visualization

Slides are mounted and coverslipped using a drop Citifluor AF1 (Agar
  ↪ Scientific, R1323).

Sup3. HE staining

The series of incubations involved in performing an HE stain should be
  ↪ prepared in individual slide staining dishes before the first
  ↪ incubation with xylene is initiated. Slides should be processed in
  ↪ batches using a slide staining holder. Note that this method is
  ↪ based on a modified version of the one described in the instructions
  ↪ manual provided with Shandon Instant Hematoxylin.

1. Five minutes in hematoxylin
2. One minute in distilled water
3. 15 seconds in acidic alcohol
4. One minute in distilled water
5. One minute in bluing reagent
6. One minute in distilled water
7. One minute in 80\% ethanol
8. 30 seconds in alcoholic eosin
9. One minute in 95\% ethanol
10. Two minutes in 100\% ethanol

```
11. Five minutes in xylene

   Excess xylene should be allowed to evaporate in a fume hood for a few
   ↪   minutes before mounting and coverslipping.

   Slides were mounted using 100 µl Shandon ClearVue XYL (Thermo Scientific
   ↪   4212) per slide.
```

Sup4. Micrograph procesing

Slides were visualised on an Axio Imager.M2m setup, and captured in close proximity of each other. This was to allow post-capture stitching of the images. Stitcing was performed with the built-in tools provided by FIJI [S15]. Stitching was done by automation, whenever possible, but several images have been stitched by hand. There is no difference in the quality of the final image, onle in the time it takes to produce it. For a graphical overview, see Figure S2.
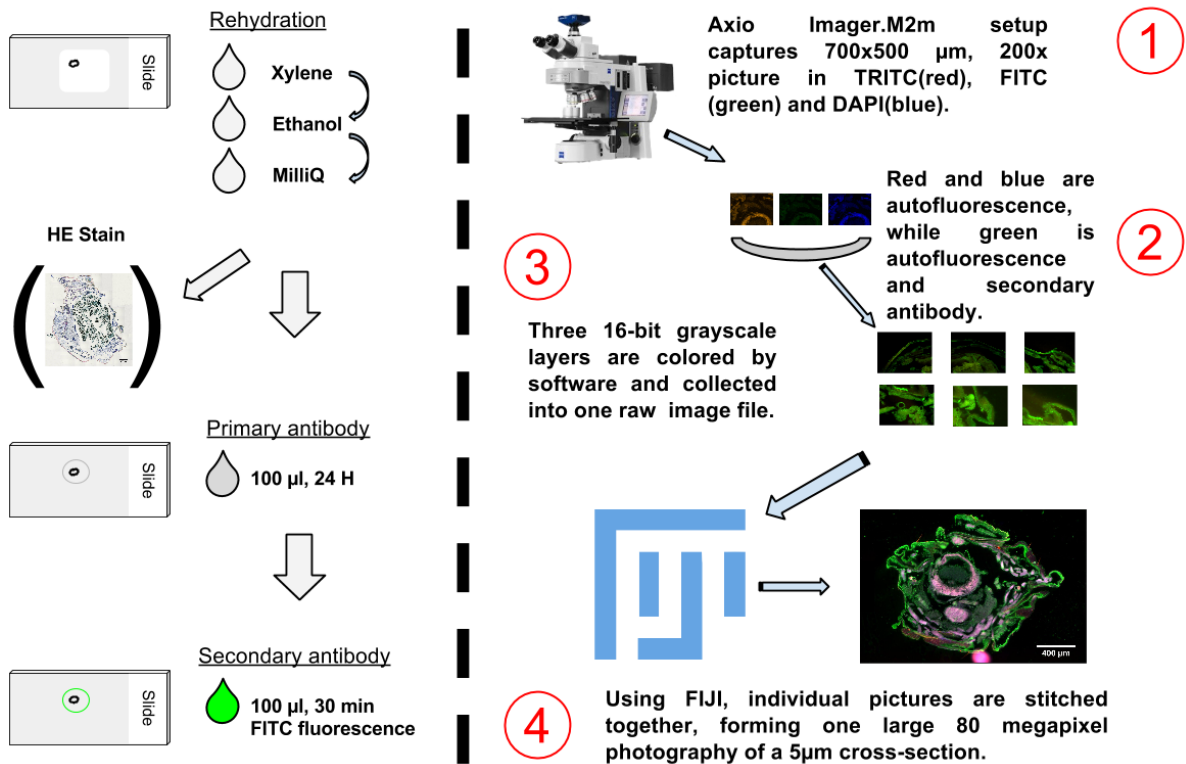
Figure S2: Overview of the slide processing method. Larva cross sections had the remaining paraffin wax removed by xylene, and were then rehydrated in increasingly hydrophilic fluids baths, going from 100 % ethanol to pure water. Slides were then incubated with the primary antibody (anti-AFP) for 24 hours, followed by buffer rinse and a thirty minute secondary antibody incubation. Slides were visualised on an Axio Imager.M2m setup, and micrographs were captured back-to-back to allow for automated image stitching. The large composite images were processed with FIJI, allowing an overview of the entire cross section, while still maintaining high resolution.

Sup5. Processing with Fiji

The fluorophore used in this study could be visualised in the green FITC range, meaning red and blue fluorescence could be considered autofluorescence. This macro function calculates the two fluorescence parameters "area" and "intensity" on a whole larva cross section. The input is a folder containing all the .tif images to be analysed. The macro runs in a vanilla version of Fiji, and only requires that the folder containing the imagery also contains two subfolders named "bin" and "jpg". These folders contain the results after analysis has ended. For a graphical overview, see Figure S3.
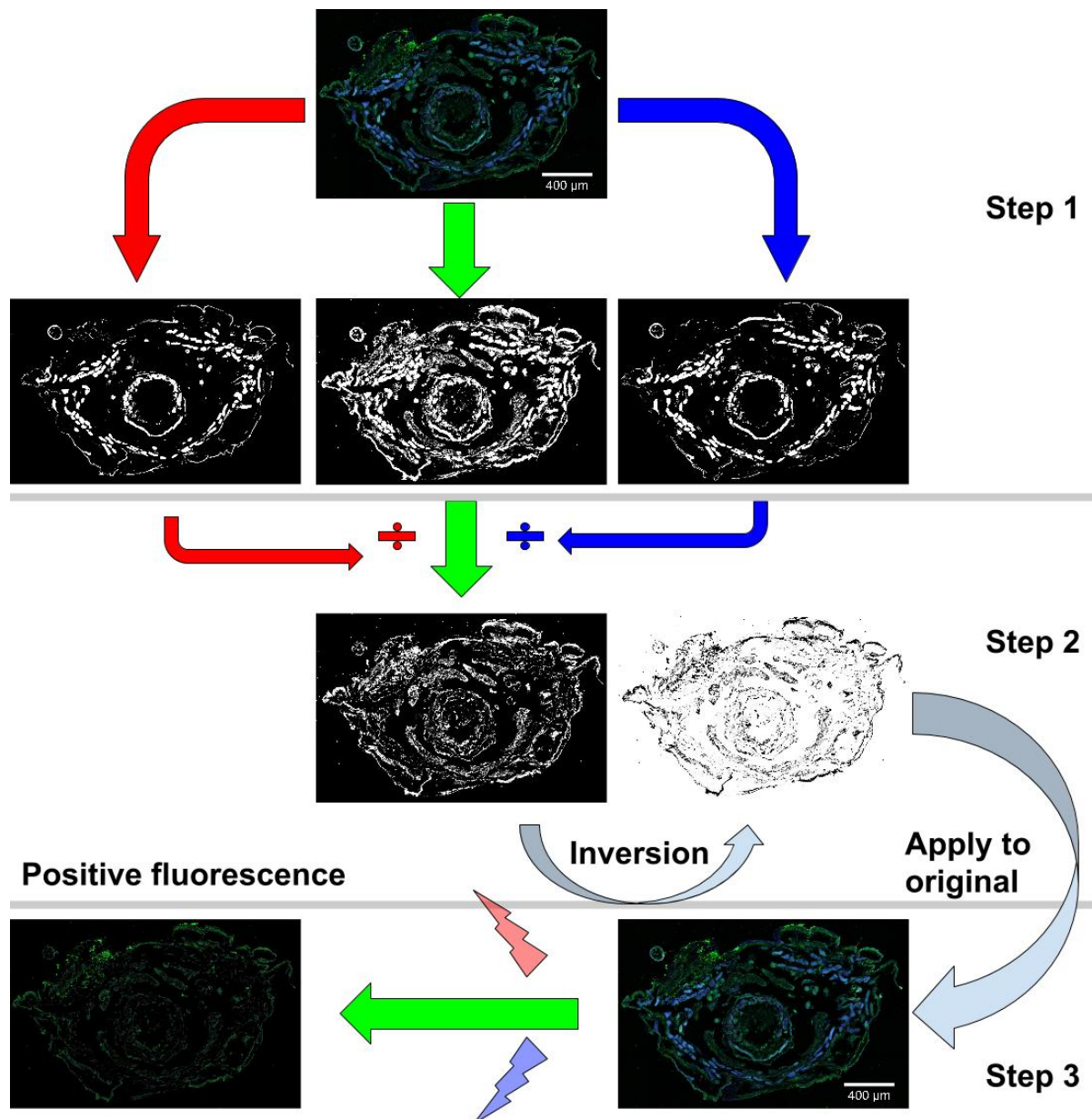
Figure S3: Graphical overview of the image processing script. The high resolution, stitched micrographs that make up the raw data in this study, have colour information in three separate layers. Antifreeze proteins were stained with a green fluorophore, so the red and blue layers are autofluorescence. Step one in the macro, is to create a binary mask of all the autofluorescence from the red and blue layer. These binary masks are then subtracted from the green layer, essentially filtering out all fluorophore fluorescence, which would have otherwise been insignificant due to autofluorescence. In step 2, the remaining green area is turned in to a binary mask. The FITC fluorescence intensity in the area covered by this mask, is the result parameter "intensity". The size of the remaining green mask, compared to the original, is the result parameter called "area". The remaining mask is then inverted, so that it covers all the areas of non-significant fluorescence. The third step is to apply the inverted mask to the original image and remove all non-significant pixels. The remaining image contains only significant fluorescence, and control images should be close to all black, like the the image seen in 4d .

```
macro "Fluorescence subtraction with area" {
dir = getDirectory("Input directory");
list = getFileList(dir);
  threshold = "unknown";
  Dialog.create("Input lower bounds");
  Dialog.addString("Threshold:", threshold);
  Dialog.show();
  threshold = Dialog.getString();

setBatchMode(true);
for (i = 0; i < list.length; i++) {
        showProgress(i+1, list.length);
filename = dir + list[i];
 if (endsWith(filename,".tif")) {
open(filename);
  name = getTitle;
  index = lastIndexOf(name, ".");
  colors = nSlices;
  if (index!=-1) name = substring(name, 0, index);
  namebin = name + "bin.txt";
  namecol = name + "col.txt";
  namejpg = name + ".jpg";
  nametwo = name + "chan2.jpg";
  bindir = dir + "/bin/";
  coldir = dir + "/col/";
  jpgdir = dir + "/jpg/";

rename("org");
selectWindow("org");

run("Set Scale...", "distance=1.98 known=1 unit="+ fromCharCode(181) + "m");
run("Scale Bar...", "width=400 height=60 font=200 color=White background=None location=[Lower Right] overlay");
saveAs("Jpeg", jpgdir+namejpg);

run("Duplicate...", "title=dup duplicate");

selectWindow("dup");

Stack.setDisplayMode("color");
setThreshold(threshold, 60000);
setOption("BlackBackground", false);
run("Make Binary", "method=Default background=Dark");
//run("Convert to Mask", "method=Default background=white");

run("Set Measurements...", "area mean standard redirect=None decimal=3");

Stack.setChannel(1);
run("Create Selection");
run("Make Inverse");
roiManager("Add");

if (nSlices==3){
Stack.setChannel(3);
run("Create Selection");
run("Make Inverse");
roiManager("Add");
}

Stack.setChannel(2);
run("Select All");
run("Create Selection");
run("Make Inverse");
roiManager("Add");
run("Measure");

roiManager("Select", 0);
```

S8

```
Stack.setChannel(2);
run("Multiply...", "value=0");

if (nSlices==3){
roiManager("Select", 1);
Stack.setChannel(2);
run("Multiply...", "value=0");
}

roiManager("Select", 0);
roiManager("Delete");
roiManager("Select", 0);
roiManager("Delete");

if (nSlices==3){
roiManager("Select", 0);
roiManager("Delete");
}

selectWindow("dup");
Stack.setChannel(2);
run("Create Selection");
run("Make Inverse");
roiManager("Add");

selectWindow("org");
roiManager("Select", 0);
run("Measure");

saveAs("Results", bindir+namebin);

selectWindow("org");
roiManager("Select", 0);
run("Make Inverse");
roiManager("Add");
roiManager("Select", 1);
run("Multiply...", "value=0 stack");
run("Select All");

run("Set Scale...", "distance=1.98 known=1 unit="
+ fromCharCode(181) + "m");
run("Scale Bar...", "width=400 height=60 font=200 color=White background=None location=[Lower Right] overlay");
saveAs("Jpeg", jpgdir+nametwo);

roiManager("Select", 0);
roiManager("Delete");
roiManager("Select", 0);
roiManager("Delete");

    if (isOpen("Results")) {
        selectWindow("Results");
        run("Close");
    }

run("Close All");
 }
}
}
```

1   This macro is similar to the previous one, in that it calculates "area" and "intensity".
2   But the input is a selection of an image, not an entire folder of images. This macro was
3   used to quantify fluorescence in gut and cuticle.

```
macro "Fluorescence subtraction with area - Selection only" {
```

S9

```
setBatchMode(true);
dir = getDirectory("Input directory");
name = getTitle;

    index = lastIndexOf(name, ".");

    if (index!=-1) name = substring(name, 0, index);

    sample = "unknown";
    Dialog.create("New Image");
    Dialog.addString("Sample:", sample);
    Dialog.show();
    sample = Dialog.getString();


    colors = nSlices;

    namesample = name + sample;
    namebin = namesample + ".txt";

    namejpg = namesample + ".jpg";
    nametwo = namesample + "chan2.jpg";
    bindir = dir + "/bin/";
    coldir = dir + "/col/";
    jpgdir = dir + "/jpg/";


roiManager("Add");

roiManager("Select", 0);

run("Duplicate...", "title=dup duplicate");

roiManager("Select", 0);
roiManager("Delete");

selectWindow("dup");
run("Select All");
run("Duplicate...", "title=dup2 duplicate");
selectWindow("dup");

Stack.setDisplayMode("composite");

run("Set Scale...", "distance=1.98 known=1 pixel=1 unit="+ fromCharCode(181) + "m");
run("Scale Bar...", "width=200 height=30 font=100 color=White background=None location=[Lower Right] overlay");

saveAs("Jpeg", jpgdir+namejpg);

Stack.setDisplayMode("color");
setThreshold(50, 60000);
setOption("BlackBackground", false);
run("Make Binary", "method=Default background=Dark");

run("Set Measurements...", "area mean standard redirect=None decimal=3");

Stack.setChannel(1);
run("Create Selection");
run("Make Inverse");
roiManager("Add");

if (nSlices==3){
Stack.setChannel(3);
run("Create Selection");
run("Make Inverse");
roiManager("Add");
}
```

S10

```
Stack.setChannel(2);
run("Create Selection");
run("Make Inverse");
roiManager("Add");
run("Measure");

roiManager("Select", 0);
Stack.setChannel(2);
run("Multiply...", "value=0 stack");

if (nSlices==3){
roiManager("Select", 1);
Stack.setChannel(2);
run("Multiply...", "value=0 stack");
}

roiManager("Select", 0);
roiManager("Delete");
roiManager("Select", 0);
roiManager("Delete");

if (nSlices==3){
roiManager("Select", 0);
roiManager("Delete");
}

Stack.setChannel(2);
run("Create Selection");
run("Make Inverse");
roiManager("Add");

selectWindow("dup");
        run("Close");

selectWindow("dup2");
run("Set Scale...", "distance=1.98 known=1 pixel=1 unit=" + fromCharCode(181) + "m");
Stack.setChannel(2);
roiManager("Select", 0);

run("Measure");
saveAs("Results",bindir+namebin);

run("Make Inverse");
run("Multiply...", "value=0 stack");

run("Scale Bar...", "width=200 height=30 font=100 color=White background=None location=[Lower Right] overlay");
run("Select All");
saveAs("Jpeg", jpgdir+nametwo);

roiManager("Select", 0);
roiManager("Delete");

   if (isOpen("Results")) {
       selectWindow("Results");
       run("Close");
   }

 }
```